

Supporting Information

High-Safety and High-Efficiency Electrolyte Design for 4.6 V-class Lithium-Ion Batteries with Non-Solvating Flame-Retardant

Li Chen^{a, b}, Qingshun Nian^a, Digen Ruan^a, Jiajia Fan^a, Yecheng Li^a, Shunqiang Chen^a, Lijiang Tan^a, Xuan Luo^a, Zhuangzhuang Cui^a, Yifeng Cheng^c, Changhao Li^c and Xiaodi Ren^{a, *}

^a School of Chemistry and Materials Science, University of Science and Technology of China, Anhui 230026, China

^b Key Laboratory of Structure and Functional Regulation of Hybrid Materials, Anhui University, Ministry of Education, Hefei, 230601, China

^c State Grid Anhui Electric Power Research Institute

Corresponding author email: xdren@ustc.edu.cn

Table S1 Abbreviation and composition of studied electrolytes.

Abbreviation	composition
E-carbonate	1M LiPF ₆ EC/EMC/DEC (1:1:1 by Vol%)
E-conc	LiFSI:DME:FEC (1:1.5:0.5 by molar ratio)
E-TMP	LiFSI:DME:FEC:TMP (1:1.5:0.5:1 by molar ratio)
E-TEP	LiFSI:DME:FEC:TEP (1:1.5:0.5:1 by molar ratio)
E-TMP-3	LiFSI:DME:FEC:TMP (1:1.5:0.5:3 by molar ratio)
E-TEP-3	LiFSI:DME:FEC:TEP (1:1.5:0.5:3 by molar ratio)
E-PFPN	LiFSI:DME:FEC:PFPN (1:1.5:0.5:3 by molar ratio)

Table S2 Physical properties of different electrolytes.

Electrolytes	Mass ratio	Molality mol/kg	Ionic conductivity (mS cm ⁻¹) at 25 °C/50°C	Viscosity (cP)	Flash Point (°C)
E-conc	1:0.72:0.28(LiFSI:DME:FEC)	2.66	6.73/10.27	24.83	72
E-TMP	1:0.72:0.28:0.75(LiFSI:DME:FEC:TMP)	1.94	7.77/12.12	13.26	47
E-PFPN	1:0.72:0.28:4.4(LiFSI:DME:FEC:PFPN)	0.83	2.22/3.42	4.32	No flash point detected

Table S3 Dielectric constant of different solvents and miscibility in electrolyte.

Solvent	Dielectric constant	Miscibility (Yes or No)
Diethyl carbonate (DEC)	2.82	Yes
Ethyl Methyl Carbonate (EMC)	2.40	Yes
Tetrahydrofuran (THF)	7.58	Yes
1,2-Dimethoxyethane (DME)	7.20	Yes
γ -butyrolactone	39.10	No
Sulfolane (SL)	43.30	No
Dimethyl Sulfoxide (DMSO)	46.68	No
Ethylene carbonate (EC)	89.60	No
Fluoroethylene carbonate (FEC)	110.00	No

Note: LiFSI:Solvent:PFPPN (1:2:3 by molar ratio)

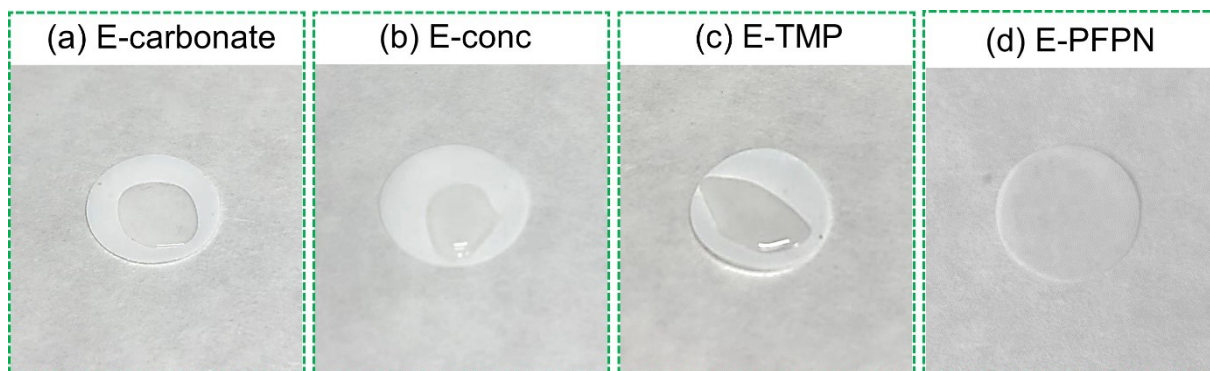


Fig. S1 Wettability tests of various electrolytes on the Celgard separator: (a) E-carbonate, (b) E-conc, (c) E-TMP, and (d) E-PFPN.

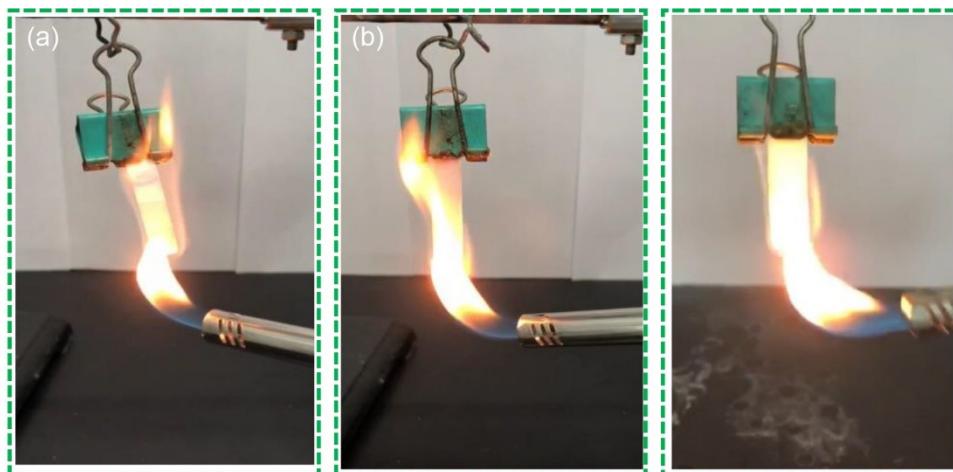


Fig. S2 Photos of ignition tests of glass fibers soaked with the (a) E-carbonate, (b) E-TEP, and E-TMP-3.

Note: In Fig. S2, The E-carbonate is extremely flammable due to the abundance of organic solvent molecules. Consistent with E-TMP electrolyte, the E-TEP cannot be ignited in a short time. However, it will also form large flames during the ignition experiment.

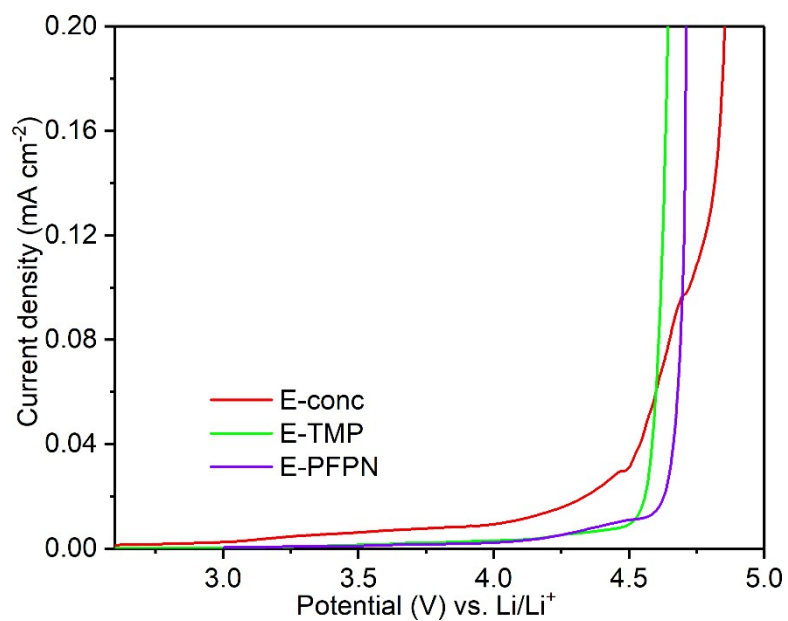


Fig. S3 Oxidation stability tests of the E-conc, E-TMP, and E-PFPN on Super-P electrode using LSV (0.1 mV s⁻¹).

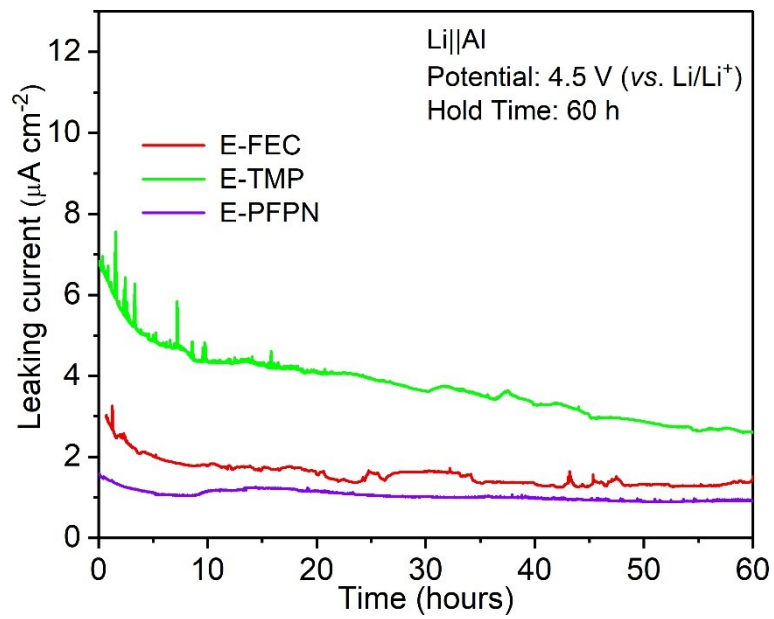


Fig. S4 Leakage currents during Al corrosion in different electrolytes at 4.5 V (vs. Li/Li⁺) for 60 h.

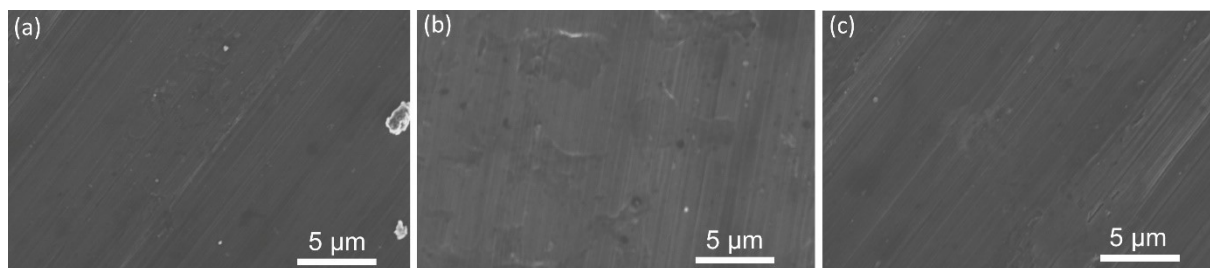


Fig. S5 Micrographs of Al electrodes being charged from OCV to 4.5 V vs. Li/Li⁺ and holding at 4.5 V in (a) E-conc, (b) E-TMP, and (c) E-PFPN for 60 h in Li||Al cells (scan rate of 0.1 mV s⁻¹).

Fig. S5 shows the SEM images of Al electrodes after being polarized from OCV to 4.5 V vs. Li/Li⁺ in various electrolytes and held at 4.5 V for 60 h in Li||Al cells. In the E-TMP, a significant number of irregular bulges can be observed on the Al current collector, which originates from the anodic dissolution of Al. However, the surface of the Al current collector is regular and flat in the E-conc and E-PFPN, illustrating the anodic dissolution of Al has been effectively suppressed in HCE and LHCE.

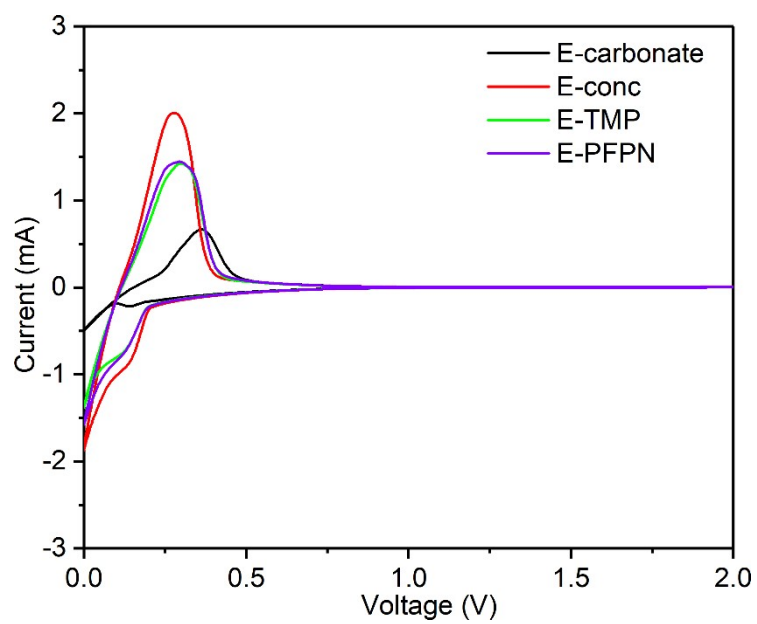


Fig. S6 The CV curves of Li||Gr cells in carbonate, E-conc, E-TMP, E-PFPN. The scan rate is 0.1 mV s^{-1} .

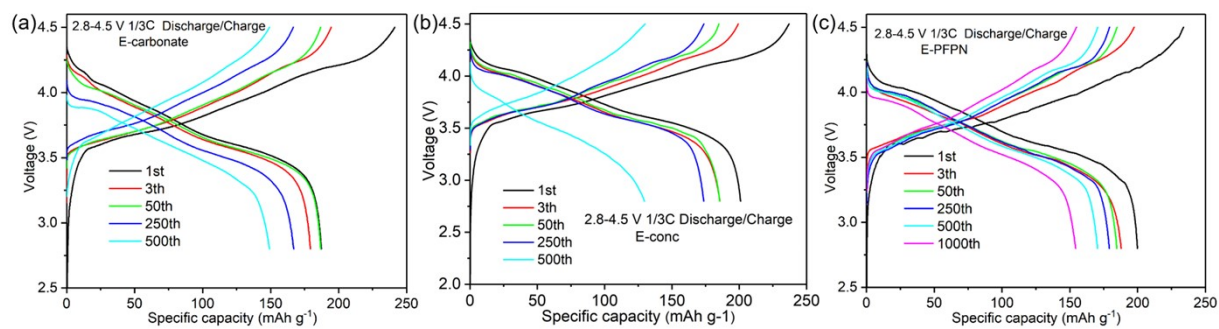


Fig. S7 Voltage profiles of the Gr||NMC811 cells at 2.8-4.5 V in (a) E-carbonate, (b) E-conc, and (c) E-PFPN.

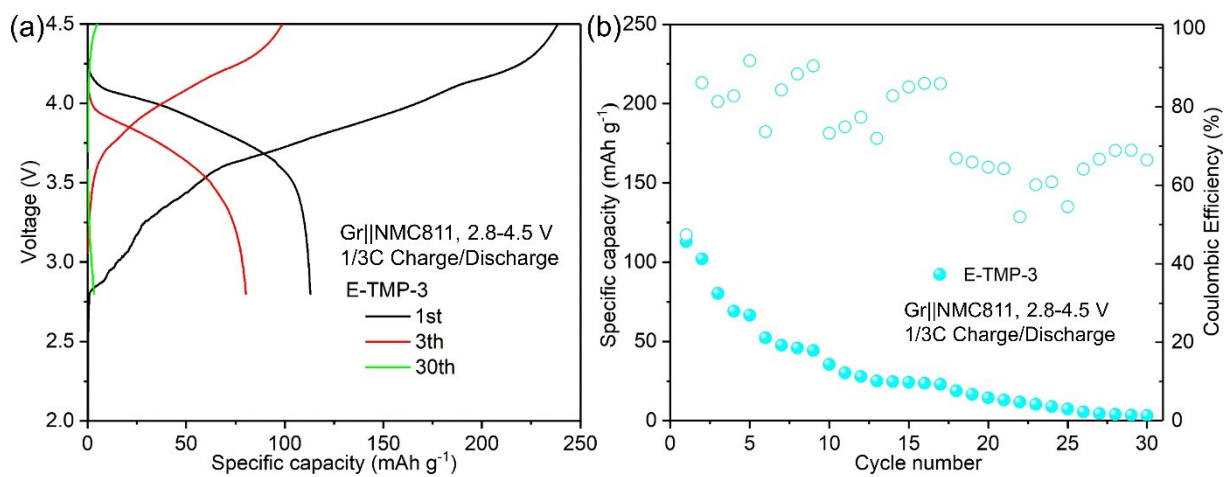


Fig. S8 (a) Voltage profiles of the Gr||NMC811 cells at 2.8-4.5 V in E-TMP-3. (b) Cycling stabilities of E-TMP-3 at 1/3C Charge/Discharge rate and a cut-off voltage of 4.5 V (25 °C).

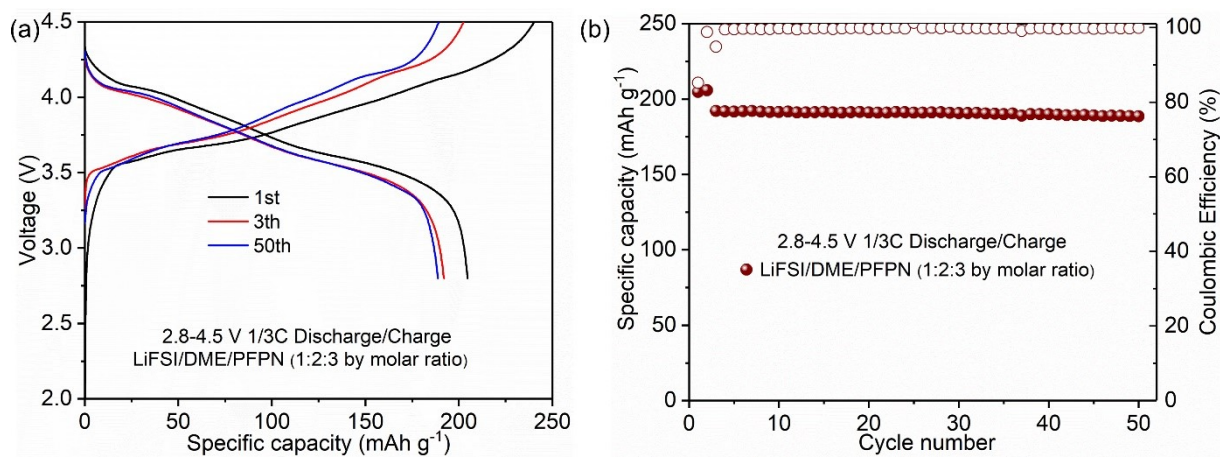


Fig. S9 (a) Voltage profiles of the Gr||NMC811 cells at 2.8-4.5 V in LiFSI/DME/PFPN. (b) Cycling stabilities of LiFSI/DME/PFPN at 1/3C Charge/Discharge rate and a cut-off voltage of 4.5 V (25 °C).

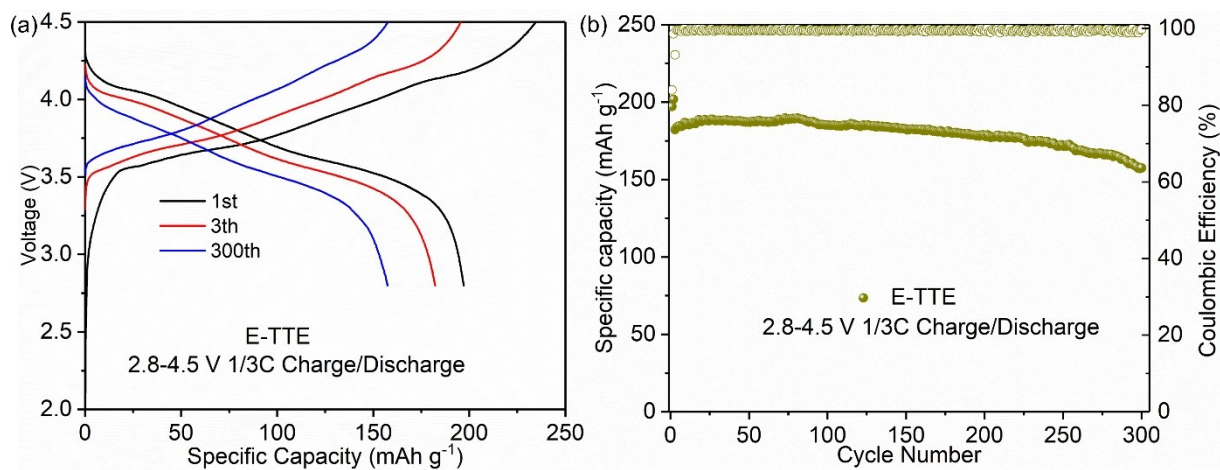


Fig. S10 (a) Voltage profiles of the Gr||NMC811 cells at 2.8-4.5 V in E-TTE. (b) Cycling stability of E-TTE at 1/3C Charge/Discharge rate under 25 °C and a cut-off voltage of 4.5 V (25 °C).

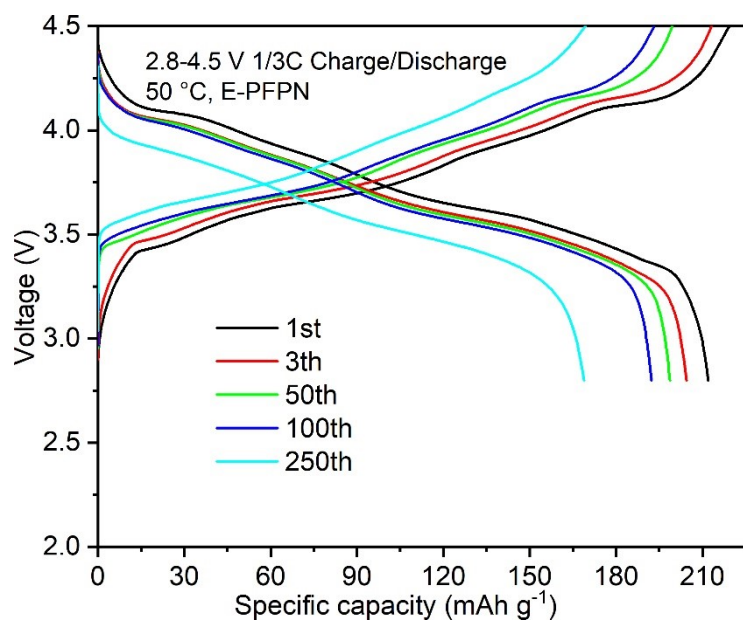


Fig. S11 Voltage profiles of the Gr||NMC811 cells at 2.8-4.5 V in E-PFPN at 1/3C Charge/Discharge rate under 50 °C.

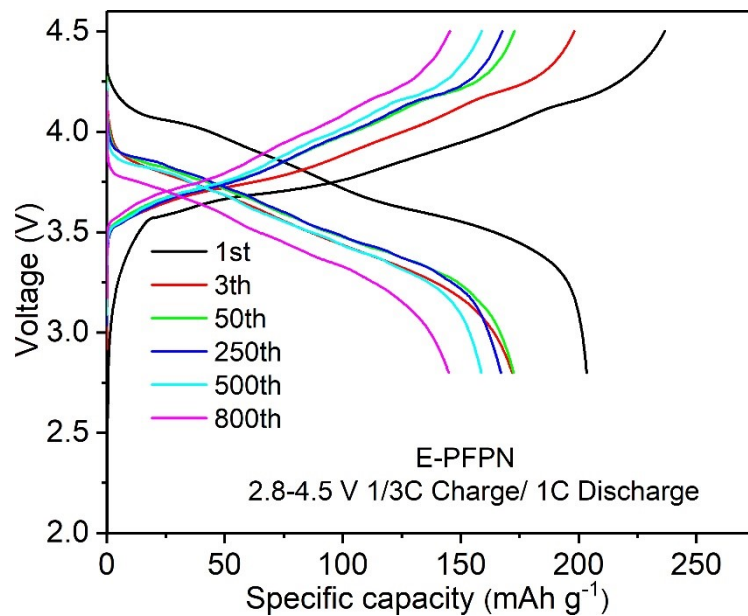


Fig. S12 Voltage profiles of the Gr||NMC811 cells at 2.8-4.5 V in E-PFPN at 1/3C Charge/ 1C Discharge rate under 25 °C.

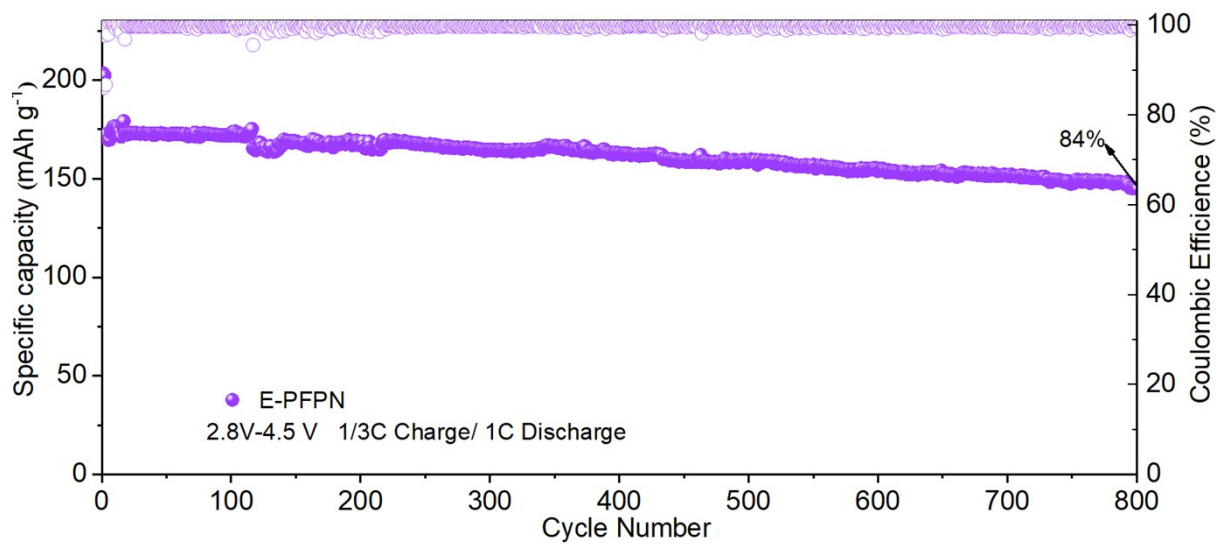


Fig. S13 Cycling stabilities of Gr||NMC811 cells in E-PFPN at 1/3C charge/ 1C discharge rate and a cut-off voltage of 4.5 V under 25 °C (the cells cycled at 0.1 C for the two formation-cycle).

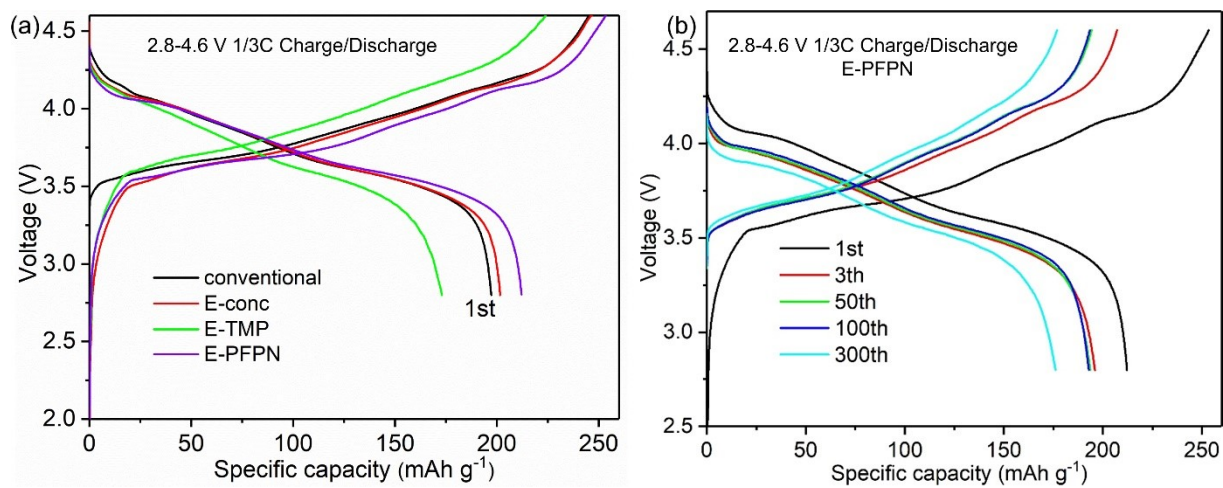


Fig. S14 (a) Voltage profiles of the Gr||NMC811 cells at 2.8-4.6 V in various electrolytes at first cycle. (b) Voltage profiles of the Gr||NMC811 cells at 2.8-4.6 V in E-PFPN.

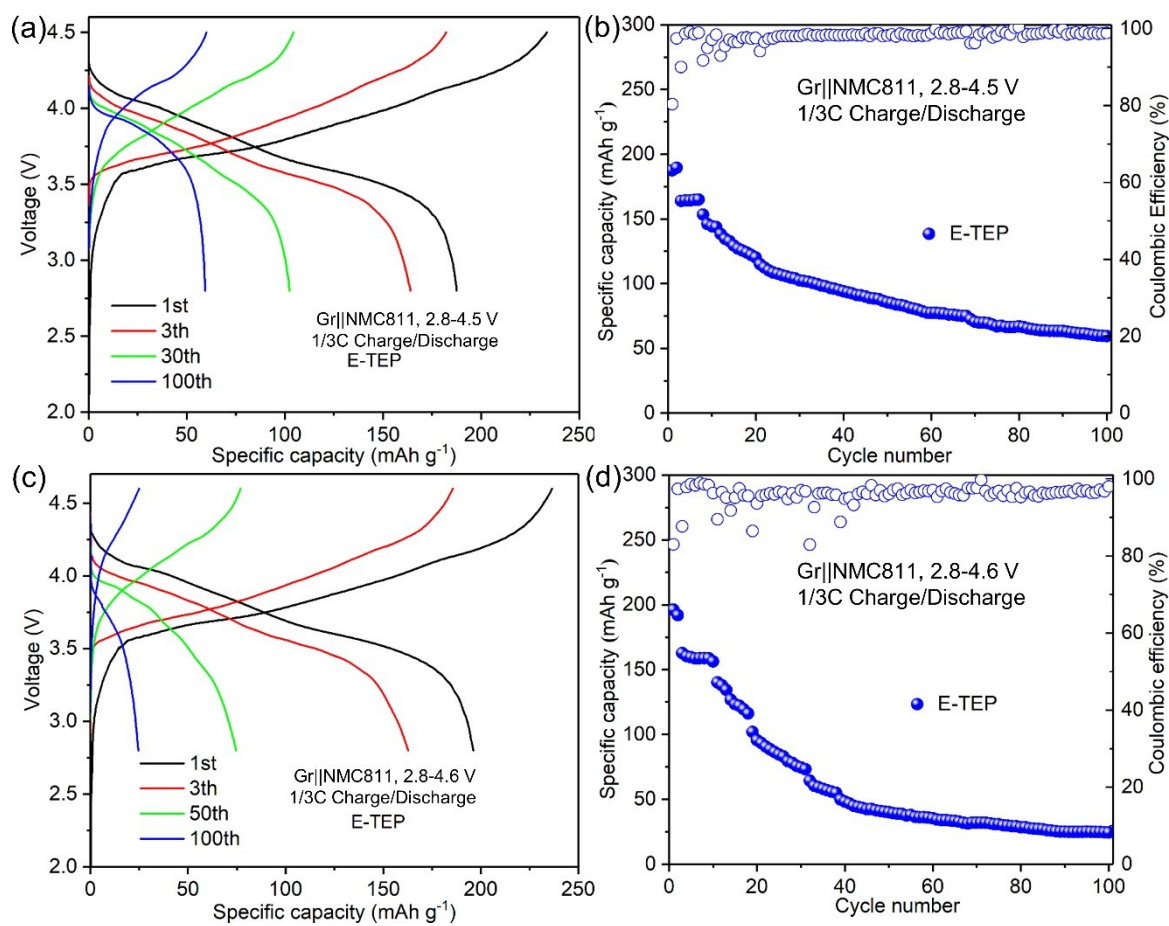


Fig. S15 Voltage profiles of the Gr||NMC811 cells in E-TEP under (a)-(b) 2.8-4.5 V and (c)-(d) 2.8-4.6 V.

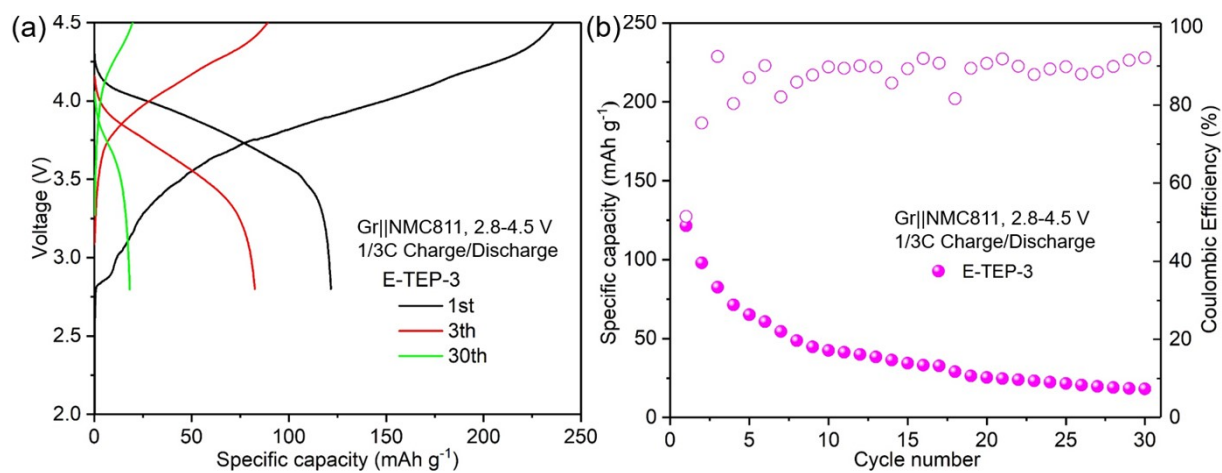


Fig. S16 (a) Voltage profiles of the Gr||NMC811 cells at 2.8-4.5 V in E-TEP-3. (b) Cycling stabilities of E-TEP-3 at 1/3C Charge/Discharge rate and a cut-off voltage of 4.5 V (25 °C).

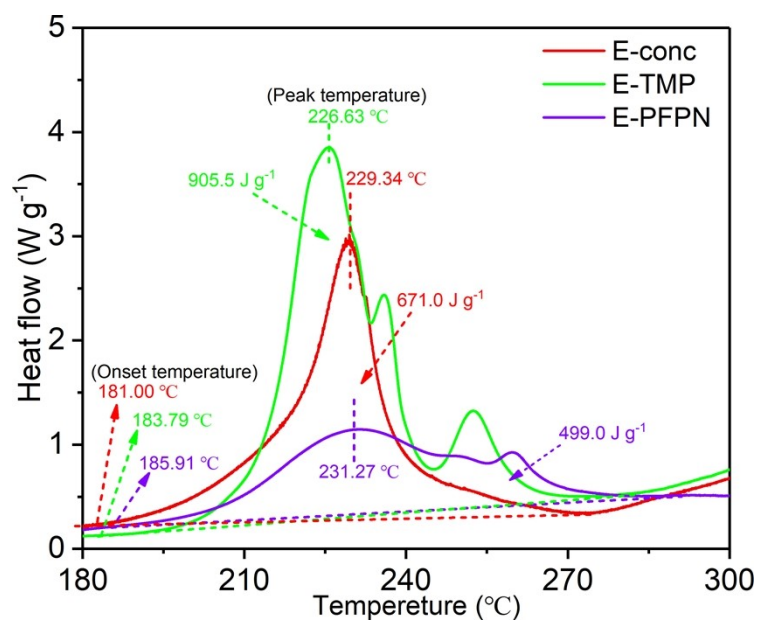


Fig. S17 DSC profiles of NMC811 cathode charged to 4.5 V combined with different electrolyte.

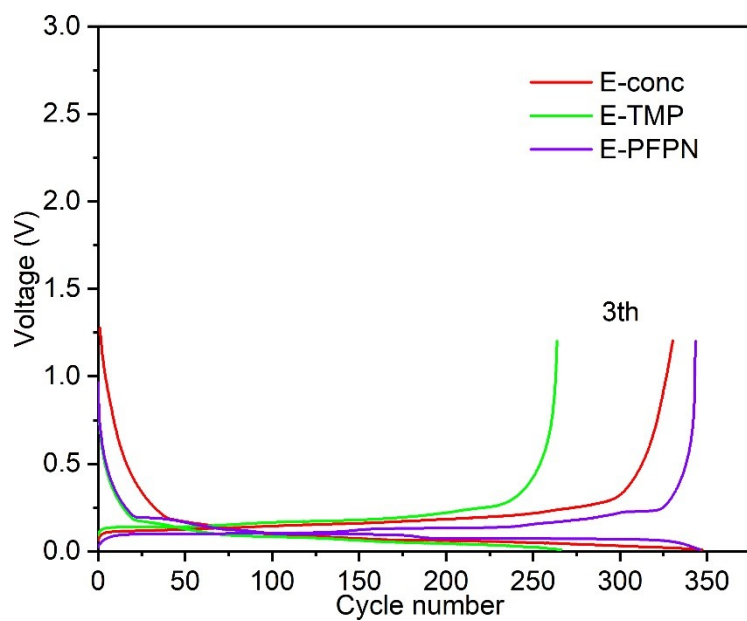


Fig. S18 The 3rd cycle charge/discharge voltage curves of various electrolytes (E-conc, E-TMP, and E-PFPN) in Li||Gr half cells at 1/5C with the cutoff voltage range of 0.01-1.2 V and $1C=372 \text{ mAh g}^{-1}$ based on the weight of the Gr active material.

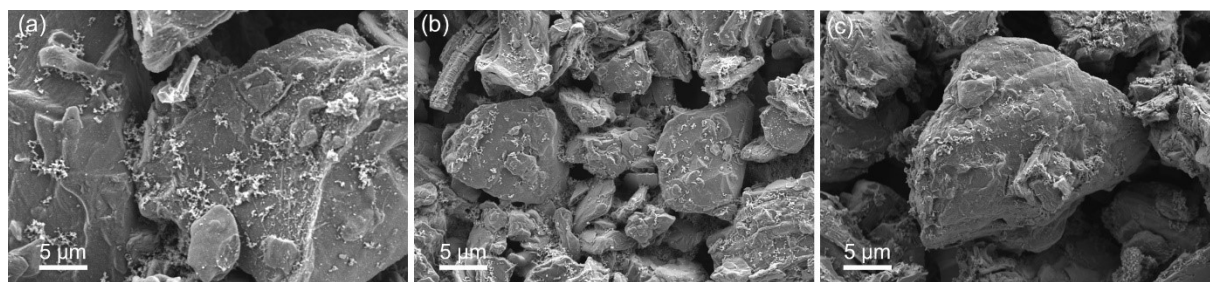


Fig. S19 SEM images of Gr anode after cycling for 50 cycles in different electrolytes. (a) E-conc, (b) E-TMP, and (c) E-PFPN.

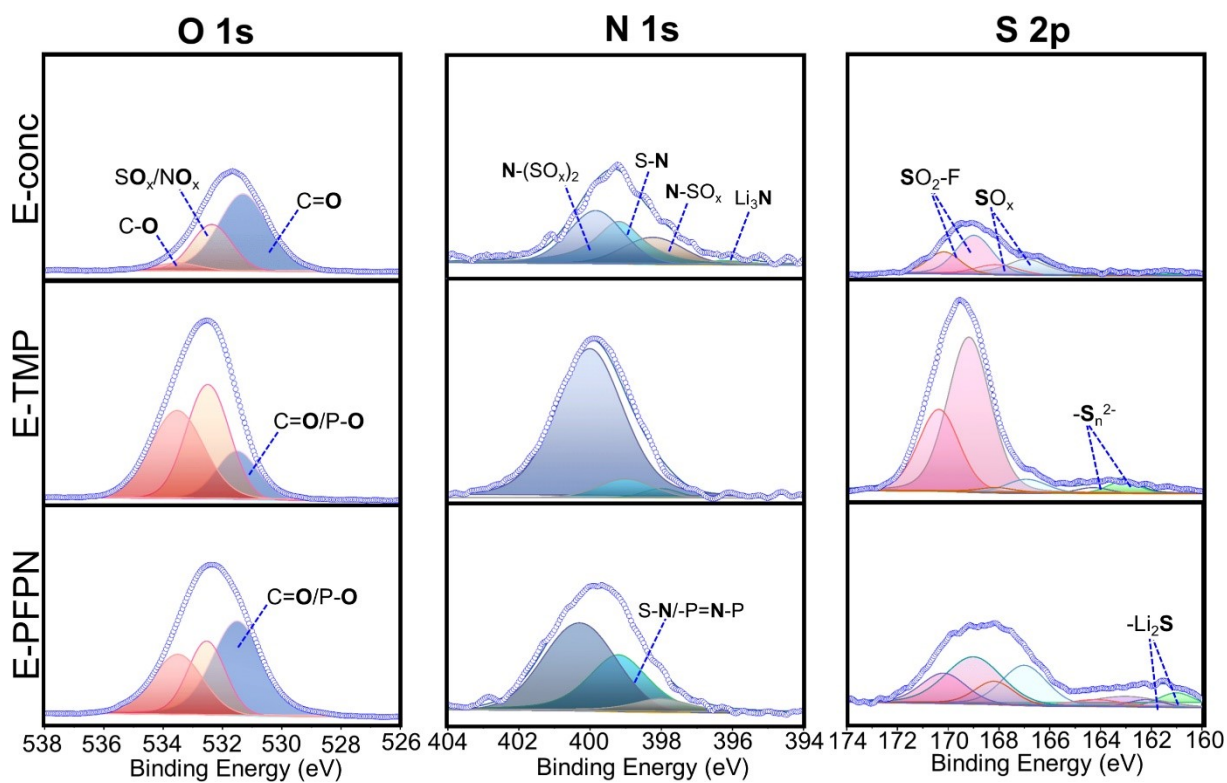


Fig. S20 XPS spectra of selected elements of the SEI on Gr electrodes received from the Gr||NMC811 cells after 50 charge/discharge cycles in the studied electrolytes: (a) O 1s, (b) N 1s, and (c) S 2p.

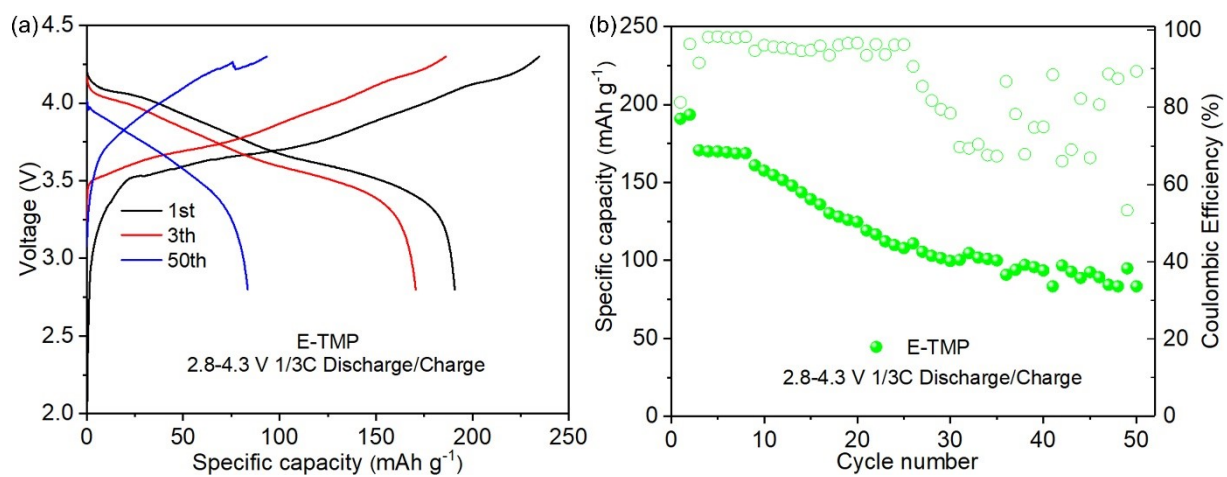


Fig. S21 (a) Voltage profiles of the Gr||NMC811 cells at 2.8-4.3 V in E-TMP. (b) Cycling stability of E-TMP at 1/3C Charge/Discharge rate and a cut-off voltage of 4.3 V (25 °C).

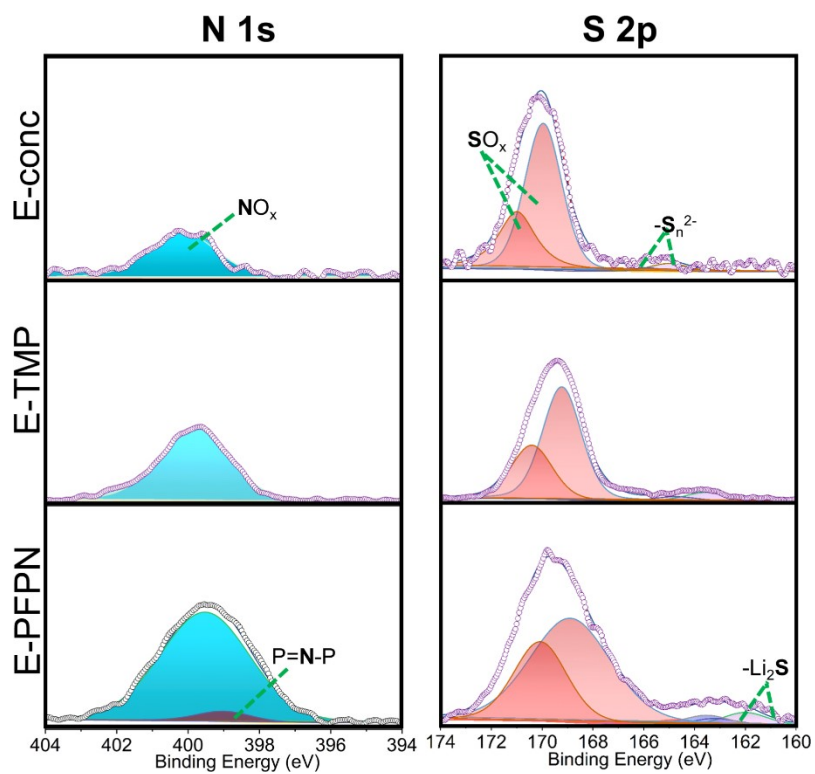


Fig. S22 XPS spectra of selected elements of the CEI on NMC811 cathode received from the Gr||NMC811 cells after 50 charge/discharge cycles in the studied electrolytes: (a) N 1s and (b) S 2p.

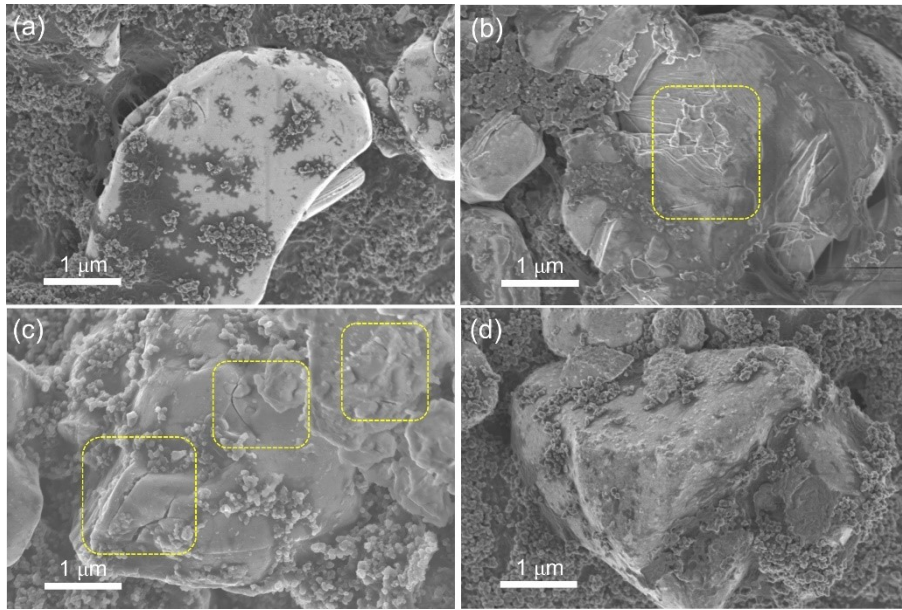


Fig. S23 SEM images of (a) pristine NMC811 and (b-d) NMC811 after cycling for 50 cycles in different electrolytes: (b) E-conc , (c) E-TMP, and (d) E-PFPN.

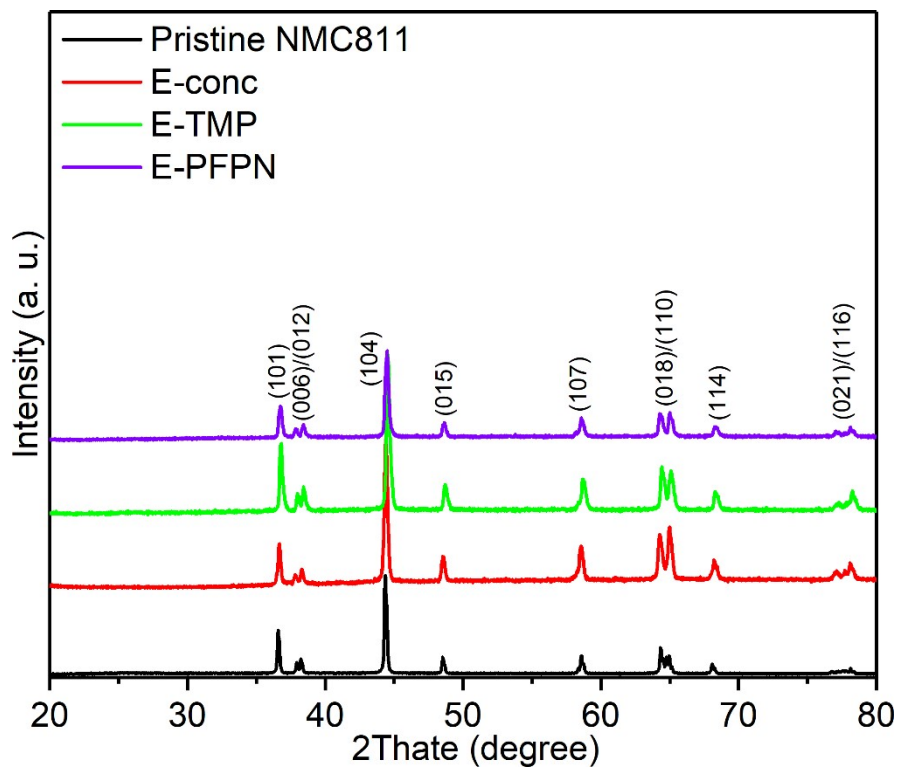


Fig. S24 XRD patterns of pristine and cycled NMC811 cathodes different electrolytes: E-conc, E-TMP, and E-PFPN.

As shown in Figure S24, the three cycled NMC811 cathodes exhibit XRD patterns similar to the pristine one. The layered structures of all the cycled cathode are largely retained after cycling from the peaks of (006)/(012).